Anticancer effects of tangeretin associated with reactive oxygen species generation, mitochondrial dysfunction and apoptosis in CaSki cells

SEUNG-HYEON AHN[1], ZEESHAN AHMAD BHUTTA[1], HWAYOUNG NA[1], HONG KYU LEE[2] and KYUNG-CHUL CHOI[1]

[1]Laboratory of Biochemistry and Immunology, College of Veterinary Medicine, Chungbuk National University, Cheongju, Chungcheongbuk 28644, Republic of Korea; [2]Department of Companion Animal Health, College of Biomedical Science and Health, Inje University, Gimhae, Gyeongsangnam 50834, Republic of Korea

Received January 23, 2026; Accepted June 15, 2026

DOI: 10.3892/or.2026.9171

Abstract. Cervical cancer is the fourth most common cancer and the fourth leading cause of cancer-related mortality among women worldwide. Tangeretin (TAN), a polymethoxylated flavonoid derived from citrus fruit peel, exhibits relatively high structural stability due to its methoxy groups and exerts anticancer effects in various malignancies, including lung, liver and breast cancer. However, to the best of our knowledge, the anticancer effects of TAN in cervical cancer remain insufficiently explored. The present study investigated the mechanisms underlying the anticancer effects of TAN on the CaSki cervical cancer cell line. Cell viability was evaluated using the EZ-Cytox cell viability assay. The colony formation and cell cycle arrest assays demonstrated that TAN inhibited cell proliferation by inducing G_1 phase arrest. The wound-healing and Transwell migration assays demonstrated that TAN could reduce the migratory ability of CaSki cells, and the Annexin V/propidium iodide staining assay revealed that TAN increased the apoptotic cell population. Mitochondrial reactive oxygen species (ROS) were identified using MitoSOX™ staining and the mitochondrial membrane potential (MMP) was detected using JC-1 staining. The findings of these assays suggested that TAN could increase mitochondrial ROS levels and decrease mitochondrial MMP in CaSki cells. Western blot analysis showed that TAN upregulated the protein expression levels of E-cadherin and Bax. In addition, TAN restored the tumor suppressor protein p53. Collectively, these findings suggested that may exhibit anticancer activity in CaSki cells.

Introduction

Cervical cancer remains one of the leading causes of cancer-related incidence and mortality among women worldwide. According to GLOBOCAN 2022 estimates, ~662,000 new cases of cervical cancer and 349,000 associated deaths were reported globally in 2022 (1). Early-stage cervical cancer is usually treated with conization; however, when early detection fails and metastasis occurs, patients require treatment with chemotherapy, with alkylating agents and antitumor antibiotics commonly used (2). However, various challenges, including the high *in vivo* toxicity of anticancer drugs and the relatively high cost of treatment, indicate that further research to improve anticancer treatment strategies is still required (3). Cervical cancer, which is primarily caused by a persistent infection with a high-risk strain of the human papillomavirus (HPV), is characterized by HPV-mediated alterations to, and functional inactivation of, tumor suppressor proteins, including p53. Accordingly, strategies aimed at restoring the activity and expression of tumor suppressor proteins may represent a promising therapeutic approach for cervical cancer (4). Notably, studies have demonstrated that phytochemicals can modulate the expression of tumor suppressor proteins in cancer cells (5,6); thus highlighting the need to evaluate the therapeutic potential of phytochemicals in the treatment of cervical cancer.

Phytochemicals are naturally occurring plant-derived compounds that exhibit relatively low biological toxicity compared with synthetic drugs (7). Because of these benefits, phytochemicals are being explored for the treatment of various

Correspondence to: Professor Kyung-Chul Choi, Laboratory of Biochemistry and Immunology, College of Veterinary Medicine, Chungbuk National University, 1 Chungdae-ro, Cheongju, Chungcheongbuk 28644, Republic of Korea
E-mail: kchoi@cbu.ac.kr

Professor Hong Kyu Lee, Department of Companion Animal Health, College of Biomedical Science and Health, Inje University, 197 Inje-ro, Gimhae, Gyeongsangnam 50834, Republic of Korea
E-mail: hklee83@inje.ac.kr

Abbreviations: DMSO, dimethyl sulfoxide; EMT, epithelial-mesenchymal transition; FBS, fetal bovine serum; HPV, human papillomavirus; MMP, mitochondrial membrane potential; PI, propidium iodide; PFA, paraformaldehyde; RPMI, Roswell Park Memorial Institute; ROS, reactive oxygen species; TAN, tangeretin

Key words: cervical cancer, CaSki, TAN, anticancer effect

diseases, including cancer and Alzheimer's disease (8,9). Phytochemicals are broadly classified into polyphenols, terpenoids, alkaloids and organosulfur compounds, each with distinct chemical structures and biological activities. Among these, polyphenols have attracted considerable attention due to their potent antioxidant and anticancer properties, and include subclasses such as flavonoids and phenolic acids (10). Flavonoids are a major class of polyphenols with a C6-C3-C6 structure and include subclasses such as flavones, flavanols, flavanones and isoflavones (11). Previous studies have reported that flavonoids exhibit antioxidant and anticancer properties in various cancer types, including breast, colorectal, lung and liver cancer, and are generally associated with low toxicity toward normal cells (12,13). However, a number of flavonoids have limited bioavailability and polymethoxylated flavonoids (PMFs) have emerged as a promising strategy to address this limitation (14,15).

Tangeretin (TAN) is a PMF found predominantly in citrus peels. It has been suggested that the multiple methoxy (-OCH_3) groups of TAN may contribute to its enhanced chemical stability and resistance to oxidative degradation compared with other flavonoids (16). According to a previous pharmacokinetic study, TAN exhibits higher bioavailability than other PMFs, including nobiletin and sinensetin, thus suggesting that TAN may possess relatively favorable pharmacokinetic properties compared with other PMFs (17). These pharmacokinetic characteristics could contribute to the biological activity of TAN in cellular systems. TAN has been reported to exert anticancer effects associated with increased intracellular reactive oxygen species (ROS) levels, apoptosis and cell cycle arrest; these effects have been observed in multiple cancer types, including lung, colon and gastric cancer (18-20). However, to the best of our knowledge, the anticancer effects of TAN on cervical cancer have not yet been elucidated, highlighting the need for further investigation. The present study aimed to evaluate the effects of TAN on cervical cancer cell viability, proliferation and migration. Furthermore, the ability of TAN to induce mitochondrial ROS generation and apoptosis was investigated, and changes in p53 protein expression following TAN treatment were examined.

Materials and methods

Chemicals. TAN (purity ≥95%) was purchased from Aladdin Scientific Corporation. A stock solution of TAN was prepared in dimethyl sulfoxide (DMSO; Sigma-Aldrich; Merck KGaA) and was subsequently diluted in culture medium to achieve the desired concentrations, with the final DMSO concentration maintained at <0.1% in all experiments.

Cell culture. CaSki cells were purchased from the Korean Cell Line Bank; Korean Cell Line Research Foundation. The cells were cultured in Roswell Park Memorial Institute (RPMI)-1640 medium (R&D Systems, Inc.) supplemented with 10% fetal bovine serum (FBS; R&D Systems, Inc.), 10 mM HEPES (Sigma-Aldrich; Merck KGaA) and 1% antibiotic-antimycotic solution (Sigma-Aldrich; Merck KGaA). Subculturing was performed using 0.05% trypsin-EDTA (Thermo Fisher Scientific, Inc.) at a split ratio of 1:5. The cells were maintained at 37˚C in a humidified incubator containing 5% CO_2.

Cell viability assays. CaSki cells were seeded in 96-well plates at a density of $4x10^3$ cells/well. After 24 h of incubation, the medium was replaced with RPMI-1640 supplemented with 5% FBS containing either 0.1% DMSO (control) or TAN (2.5-40 μM). After 48 h of treatment at 37˚C in a humidified incubator with 5% CO_2, the culture medium was removed and 5% EZ-Cytox cell viability assay reagent (cat. no. EZ-3000; DoGenBio), a water-soluble tetrazolium salt reagent, was added and incubated for 30 min at 37˚C in a humidified incubator with 5% CO_2. Absorbance was measured at 450 nm using a Synergy Neo2 Hybrid Multimode Reader (Agilent Technologies, Inc.).

Colony formation assay. CaSki cells were seeded in 6-well plates at a density of $1x10^3$ cells/well and incubated for 24 h. The cells were then treated with RPMI-1640 medium supplemented with 5% FBS containing either 0.1% DMSO (control) or TAN (10-40 μM) for 48 h at 37˚C in a humidified incubator with 5% CO_2. Thereafter, the culture medium was replaced every 3 days with RPMI-1640 supplemented with 5% FBS, and the experiment was continued for 2 weeks. For analysis, the colonies were fixed with 4% paraformaldehyde (PFA; GeneAll Biotechnology Co., Ltd.) for 15 min at room temperature and stained with 0.5% crystal violet (Sigma-Aldrich; Merck KGaA) for 30 min at room temperature. Colony formation was quantified by measuring the total colony area using ImageJ software (version 1.53; National Institutes of Health). Colonies with an area of ≥20 $pixels^2$ were included in the analysis. The colony formation rate was calculated by normalizing the colony area of each treatment group to that of the control group, which was set to 100%.

Wound-healing assay. CaSki cells were seeded in 6-well plates at a density of $1x10^5$ cells/well and incubated at 37˚C in a humidified atmosphere containing 5% CO_2 for 48 h until they reached ~80% confluence. To minimize the contribution of cell proliferation during wound closure analysis, the cells were pretreated with mitomycin C (2 μg/ml; Roche Diagnostics) for 1.5 h at 37˚C in a humidified incubator containing 5% CO_2 prior to scratch formation. A linear scratch was then generated in each well using sterile surgical forceps. After removing the culture medium and washing to eliminate cellular debris, the cells were incubated in RPMI-1640 medium supplemented with 5% FBS, containing either 0.1% DMSO (control) or TAN (1.25-5 μM). The FBS concentration (5%) was selected to maintain cell viability during the wound-healing assay (21). After treatment, the cells were incubated at 37˚C in a humidified atmosphere containing 5% CO_2. Images of the wound area were captured at 0, 24 and 48 h at x40 magnification using an Olympus CKX41 inverted light microscope (Olympus Corporation), and wound closure was semi-quantified using ImageJ software (version 1.53).

Transwell migration assay. CaSki cells ($5x10^5$ cells/well) were seeded into the upper chamber of 24-well Transwell inserts (pore size, 8.0-μm). The upper chamber was filled with RPMI-1640 medium supplemented with 1% FBS containing either 0.1% DMSO (control) or TAN (10-40 μM). The lower chamber contained RPMI-1640 medium supplemented with 10% FBS as a chemoattractant. After 48 h of incubation at 37˚C in a humidified atmosphere containing 5% CO_2, the

non-migratory cells on the upper surface of the membrane were removed, and cells that had migrated to the lower surface were fixed with 4% PFA for 15 min at room temperature and stained with 0.5% crystal violet for 30 min at room temperature. Images were captured using an Olympus CKX41 microscope, and the number of migrated cells was semi-quantified using ImageJ software (version 1.53).

Cell cycle arrest assay. CaSki cells ($3x10^3$ cells/well) were seeded in 6-well plates and incubated for 24 h. The culture medium was then replaced with RPMI-1640 supplemented with 5% FBS containing either 0.1% DMSO (control) or TAN (10-40 μM). After 48 h of treatment at 37˚C in a humidified atmosphere containing 5% CO_2, the cells were harvested and fixed in 70% ethanol at -20˚C overnight. Fixed cells were subsequently stained with Hoechst 33342 (10 μg/ml; cat. no. H3570; Thermo Fisher Scientific, Inc.) for 30 min at 37˚C in a humidified atmosphere containing 5% CO_2. Hoechst 33342, a DNA-binding fluorescent dye, was used to determine cell cycle distribution based on cellular DNA content, as previously described (22). Cell cycle distribution was analyzed using a FACSymphony™ flow cytometer (BD Biosciences) with the BV421 channel and data were analyzed using FlowJo software (version 10; BD Biosciences).

Annexin V and propidium iodide (PI) staining. CaSki cells ($3x10^3$ cells/well) were seeded in 6-well plates and incubated for 24 h. The culture medium was then replaced with RPMI-1640 supplemented with 5% FBS containing either 0.1% DMSO (control) or TAN (10-40 μM). After 48 h of treatment at 37˚C in a humidified atmosphere containing 5% CO_2, the cells were harvested and resuspended in 100 μl 1X Annexin-binding buffer. Subsequently, 5 μl Alexa Fluor™ 488 Annexin V and 1 μl PI (100 μg/ml) from the Alexa Fluor 488 Annexin V/Dead Cell Apoptosis Kit (Invitrogen; Thermo Fisher Scientific, Inc.) were added to each sample and incubated for 15 min at room temperature in the dark according to the manufacturer's instructions. Following incubation, 400 μl 1X Annexin-binding buffer was added and the samples were immediately analyzed using a FACSymphony flow cytometer and the percentage of apoptotic cells was quantified using FlowJo software (version 10).

MitoSOX™ staining. CaSki cells were seeded in 96-well plates at a density of $6x10^3$ cells/well and incubated for 24 h at 37˚C in a humidified atmosphere containing 5% CO_2. The culture medium was then replaced with RPMI-1640 supplemented with 5% FBS containing either 0.1% DMSO (control) or TAN (10-40 μM). After 48 h of treatment at 37˚C in a humidified atmosphere containing 5% CO_2, the medium was removed, and the cells were incubated with MitoSOX™ Red Mitochondrial Superoxide Indicator (5 μg/ml; cat. no. M36008; Thermo Fisher Scientific, Inc.) and Hoechst 33342 (5 μg/ml; cat. no. H3570; Thermo Fisher Scientific, Inc.) for 10 min at 37˚C. Fluorescence images were acquired using a Lionheart™ FX Automated Imaging System (BioTek; Agilent Technologies, Inc.), with Hoechst 33342 detected in the DAPI channel and MitoSOX Red detected in the RFP channel. Images were acquired using a Lionheart FX Automated Microscope (BioTek; Agilent Technologies, Inc.) and analyzed using Gen5 software (version 3.05; BioTek; Agilent Technologies, Inc.) under identical image acquisition settings. Background fluorescence was automatically corrected using the built-in background subtraction function of the instrument. MitoSOX Red fluorescence intensity was normalized to the number of Hoechst 33342-positive nuclei in each field.

JC-1 staining. CaSki cells were seeded in black 96-well plates at a density of $5x10^3$ cells/well and incubated for 24 h. The culture medium was then replaced with RPMI-1640 supplemented with 5% FBS containing either 0.1% DMSO (control) or TAN (10-40 μM). After 24 h of treatment at 37˚C in a humidified atmosphere containing 5% CO_2, the medium was removed and JC-1 dye (cat. no. ab113850; Abcam) was added to each well at a final concentration of 3 μg/ml. The cells were incubated for 30 min at 37˚C and fluorescence images were acquired using a Lionheart FX Automated Imaging System, with JC-1 monomers detected in the GFP channel and JC-1 aggregates detected in the RFP channel. Images were acquired using a Lionheart FX Automated Microscope and fluorescence intensity was quantified using Gen5 software (version 3.05) under identical image acquisition settings. Background fluorescence was automatically corrected using the built-in background subtraction function of the instrument. Mitochondrial membrane potential (MMP) was evaluated based on the ratio of JC-1 aggregate (RFP) fluorescence to JC-1 monomer (GFP) fluorescence.

Western blot analysis. Cells in the control group were cultured in RPMI-1640 supplemented with 5% FBS containing 0.1% DMSO (vehicle control), and TAN-treated cells were cultured in RPMI-1640 supplemented with 5% FBS containing TAN (20 or 40 μM) for 48 h. Total cellular proteins were extracted using PRO-PREP™ protein extraction solution (Intron Biotechnology, Inc.) supplemented with a protease inhibitor cocktail (ATTO Corporation). Protein concentrations were determined using a bicinchoninic acid (BCA) protein assay following the Sigma-Aldrich BCA protein assay protocol, using BCA solution (cat. no. B9643; Sigma-Aldrich; Merck KGaA) and 4% copper(II) sulfate solution (cat. no. C2284; Sigma-Aldrich; Merck KGaA), with bovine serum albumin (BSA; cat. no. A9418; MilliporeSigma) used as the protein standard. Western blot analysis was performed using 30 μg total protein per lane. Total proteins were separated by SDS-PAGE on 8% gels for E-cadherin and 10% gels for Bax and p53, followed by transfer onto PVDF membranes (Amersham™ Hybond™ P; cat. no. 10600023; Cytiva). The membranes were blocked with 5% BSA in Tris-buffered saline containing 0.1% Tween-20 for 1 h 30 min at room temperature. After blocking, the membranes were incubated overnight at 4˚C with primary antibodies against Bax (1:1,000; cat. no. 2772; Cell Signaling Technology, Inc.), E-cadherin (1:1,000; cat. no. 3195; Cell Signaling Technology, Inc.), p53 (1:1,000; cat. no. bs-2090R; BIOSS) and GAPDH (1:5,000; cat. no. ABS16; MilliporeSigma) diluted in 5% BSA (MilliporeSigma) in Tris-buffered saline containing 0.1% Tween-20 (cat. no. 11332465001; Roche Diagnostics). The membranes were then incubated with horseradish peroxidase (HRP)-conjugated goat anti-rabbit IgG secondary antibody (1:3,000; cat. no. 1706515; Bio-Rad Laboratories, Inc.) for 1 h at room temperature. Protein bands

were visualized using an enhanced chemiluminescence (ECL) detection reagent (Amersham™ ECL™ Select Western Blotting Detection Reagent; cat. no. RPN2235; Cytiva) and images were captured using a LuminoGraph II imaging system (Cytiva). Band intensities were semi-quantified using ImageJ software (version 1.53).

Statistical analysis. All *in vitro* experiments were performed using technical triplicates under identical experimental conditions unless otherwise specified. Data are presented as the mean ± standard deviation and were analyzed using GraphPad Prism software (version 10; Dotmatics). Statistical significance was evaluated using one-way analysis of variance followed by Dunnett's post hoc test for multiple comparisons against the control group. As the data were obtained from technical triplicates, the sample size was insufficient for reliable assessment of normality and homogeneity of variance; therefore, these tests were not consistently performed. $P<0.05$ was considered to indicate a statistically significant difference.

Results

TAN decreases the viability and proliferation of CaSki cells. Previous studies have reported that TAN suppresses cell viability in various types of cancer (23-25). In the present study, TAN treatment reduced the viability of CaSki cells (Fig. 1A). Based on the cell viability assay results, 10, 20 and 40 μM TAN were selected for subsequent experiments because these concentrations showed greater inhibitory effects on cell viability than lower concentrations and allowed the evaluation of concentration-dependent biological responses. In addition, the anti-proliferative effect of TAN in CaSki cells was evaluated using a colony formation assay (Fig. 1B), which revealed a significant reduction in colony formation area in the TAN-treated group compared with that in the control group (Fig. 1C). These results indicated that TAN may reduce cell viability by inhibiting CaSki cell proliferation.

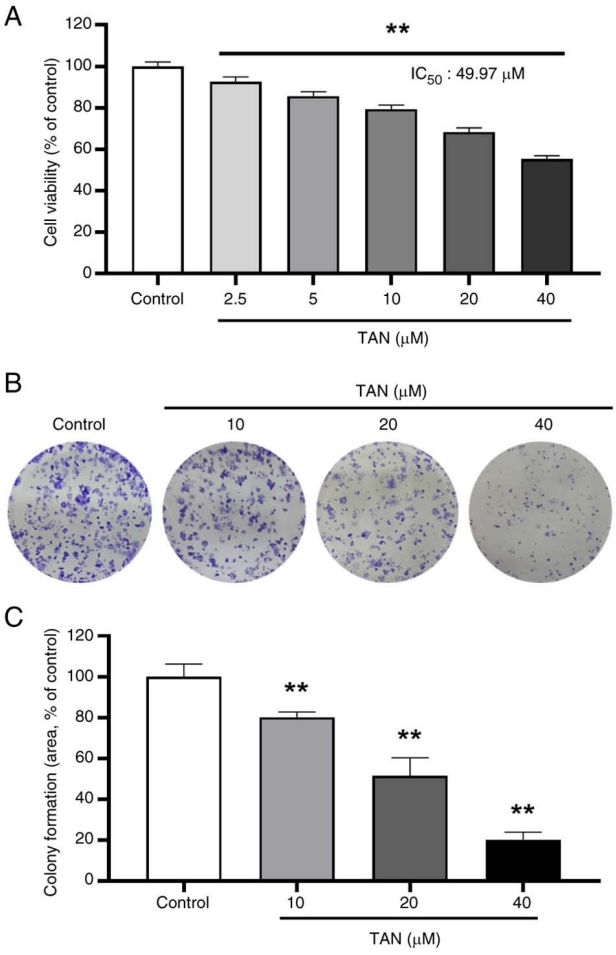

Figure 1. TAN decreases the viability and proliferation of CaSki cells. (A) Cell viability was assessed using an EZ-Cytox cell viability assay following TAN treatment. (B) Inhibitory effect of TAN on cell proliferation was assessed using a colony formation assay. (C) Colony formation was semi-quantified as the colony area and expressed as a percentage of the control. Data are presented as the mean ± SD of technical triplicates. $^{**}P<0.01$ vs. control. TAN, tangeretin.

TAN induces G_1 phase arrest in CaSki cells. TAN has been reported to suppress cancer cell proliferation primarily through the induction of G_1 phase arrest (26,27). In the current study, Hoechst 33342 staining was employed to examine cell cycle alterations associated with TAN-mediated inhibition of CaSki cell proliferation (Fig. 2A). The assay showed that TAN treatment increased the proportion of cells in the G_1 phase compared with that in the control group (Fig. 2B). These findings suggested that TAN-associated inhibition of CaSki cell proliferation may be related to G_1 phase arrest.

TAN suppresses CaSki cell migration. Effective cancer treatment requires not only the inhibition of cancer cell proliferation but also the suppression of cancer cell migration and metastasis (28). The effects of TAN on cell migration were first investigated using a wound-healing assay (Fig. 3A). Notably, TAN treatment at 5 μM significantly reduced wound closure compared with the control group at both 24 and 48 h (Fig. 3B). In addition, a Transwell migration assay was conducted to evaluate the effect of TAN on chemotactic migration (Fig. 3C). The number of migratory cells was significantly decreased in cells treated with 20 and 40 μM TAN compared with the control group (Fig. 3D). Western blot analysis was subsequently performed to detect E-cadherin (Fig. 3E). The protein expression levels of E-cadherin were increased in the TAN-treated groups compared with those in the control group (Fig. 3F). These results suggested that TAN not only inhibits the proliferation of CaSki cells, but is also associated with reduced migratory capacity and migration-associated phenotypic changes.

TAN induces intrinsic apoptosis of CaSki cells. Previous studies have reported that TAN suppresses cancer cell proliferation by inducing apoptosis, a form of programmed cell death (19,26). In the present study, apoptotic cells were analyzed by flow cytometry using Annexin V and PI staining (Fig. 4A). The proportion of apoptotic cells was significantly increased in the 20 and 40 μM TAN-treated groups compared with in the control group (Fig. 4B). Subsequently, the expression levels of the pro-apoptotic protein Bax were examined by western blotting (Fig. 4C). Bax expression was significantly

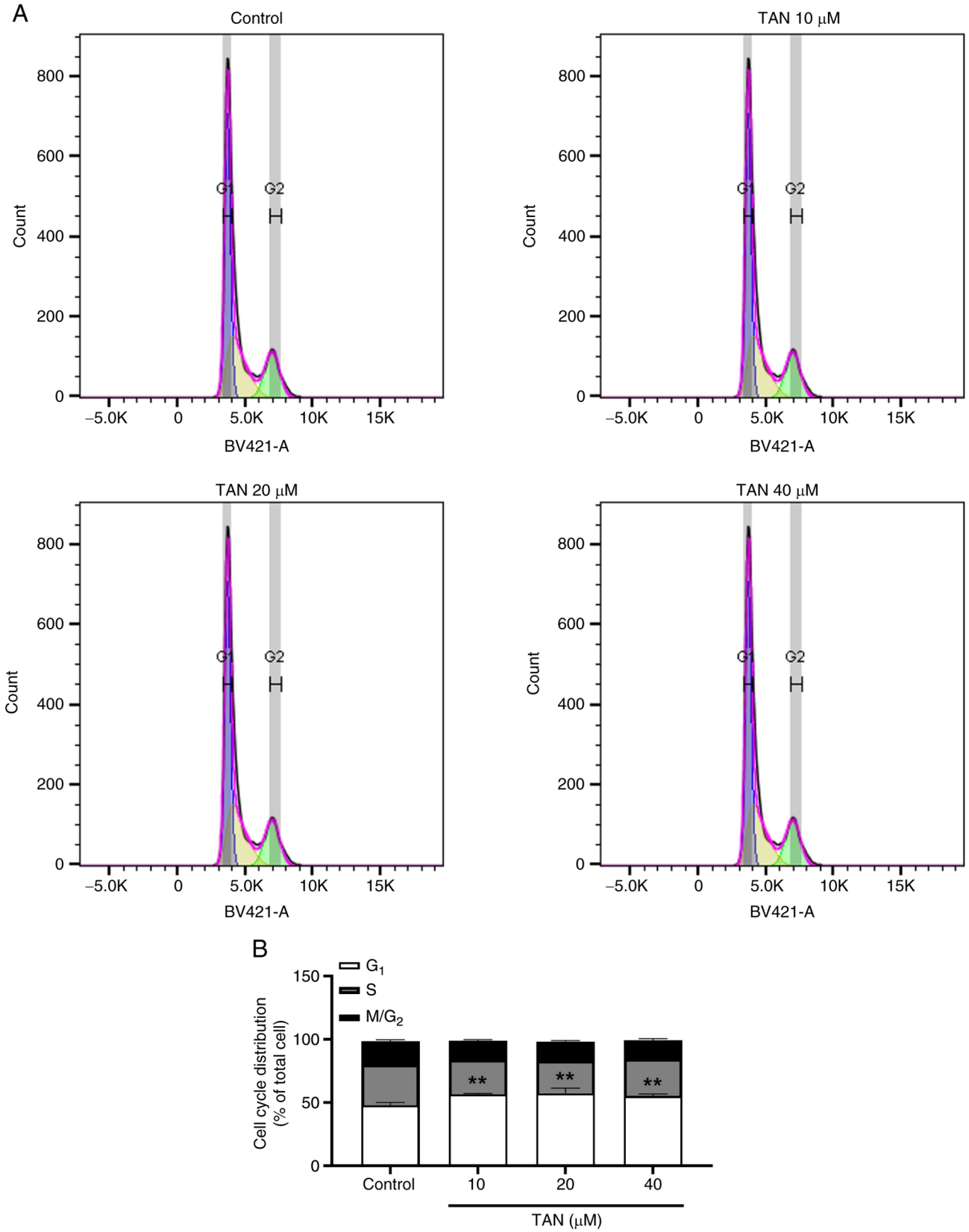

Figure 2. TAN induces G_1 cell cycle arrest in CaSki cells. (A) Cell cycle distribution was measured by flow cytometry after Hoechst 33342 staining. (B) Percentage of cells in each cell cycle phase was quantified using FlowJo software. Data are presented as the mean ± SD of technical triplicates. $^{**}P<0.01$ vs. control. TAN, tangeretin.

upregulated in the 40 μM TAN-treated group compared with in the control group (Fig. 4D). These results suggested that TAN treatment may be associated with apoptosis-related changes and increased Bax expression in CaSki cells, potentially involving the intrinsic apoptosis-associated signaling pathway.

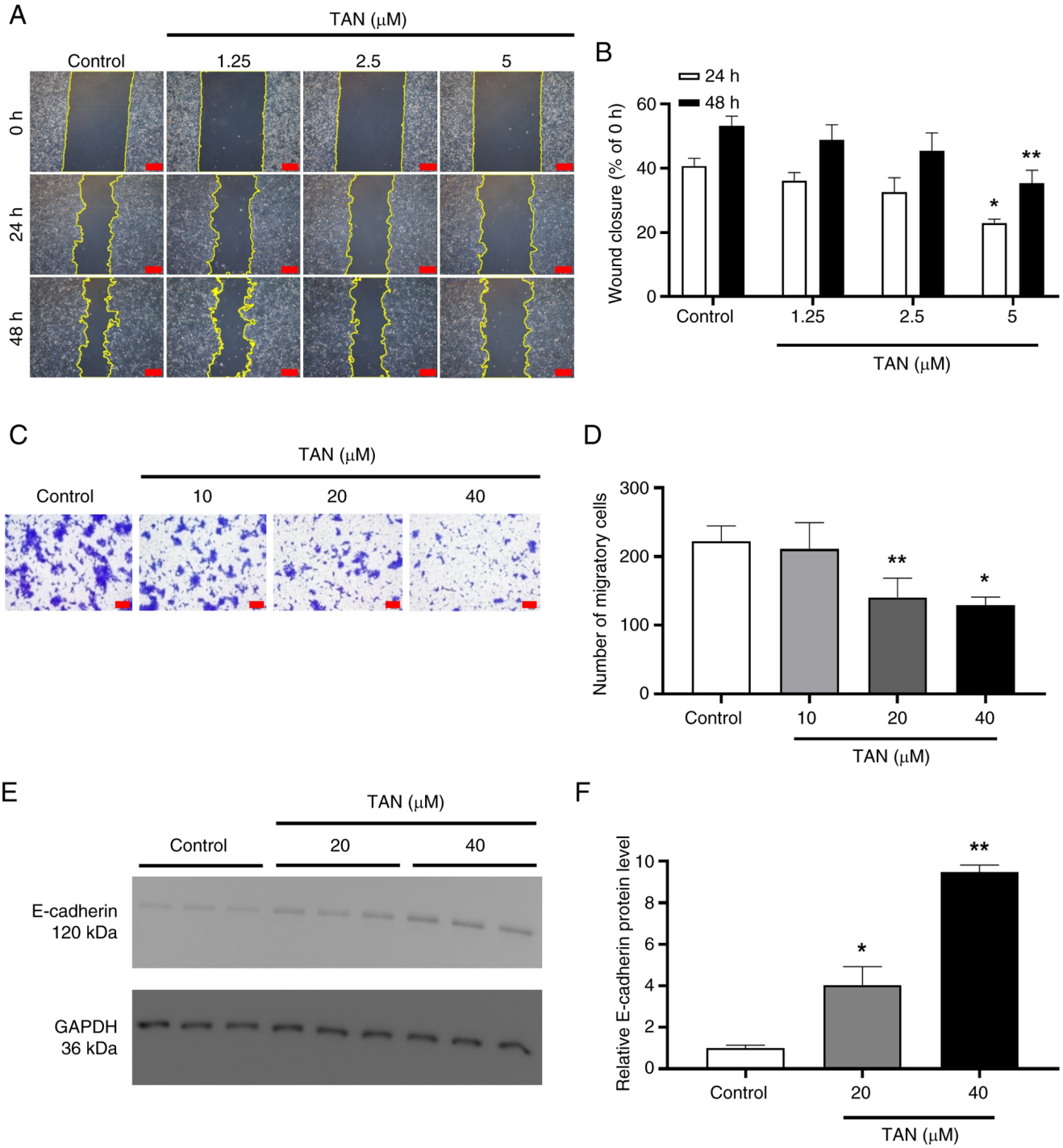

Figure 3. TAN suppresses the migratory ability of CaSki cells. (A) Representative images of the wound-healing assay showing the effect of TAN on the migration of CaSki cells. Scale bar, 500 μm. (B) Semi-quantification of wound closure at 24 and 48 h, expressed as the percentage of wound area relative to 0 h. (C) Representative images of the Transwell migration assay. Scale bar, 500 μm (D) Semi-quantification of migratory cells in the Transwell migration assay. (E) Protein expression levels of E-cadherin were analyzed by western blot analysis. (F) E-cadherin expression was semi-quantified by densitometric analysis and normalized to GAPDH. Data are presented as the mean ± SD of technical triplicates. *P<0.05, **P<0.01 vs. control. TAN, tangeretin.

TAN increases mitochondrial oxidative stress and decreases MMP in CaSki cells. TAN has been reported to exhibit various anticancer effects by increasing ROS levels in various cancer cell lines (18). The present study performed MitoSOX staining to evaluate whether TAN increases mitochondrial ROS (Fig. 5A), and observed elevated intra-mitochondrial ROS levels in the 20 and 40 μM TAN-treated groups compared with in the control group (Fig. 5B). Based on reports that excessive mitochondrial ROS in cancer cells induces changes in MMP (29), the current study further evaluated changes in MMP using JC-1 staining (Fig. 5C). The decrease in MMP was confirmed in the TAN-treated groups compared with in the control group (Fig. 5D). These findings suggested that TAN treatment is associated with increased mitochondrial ROS accumulation and decreased MMP in CaSki cells.

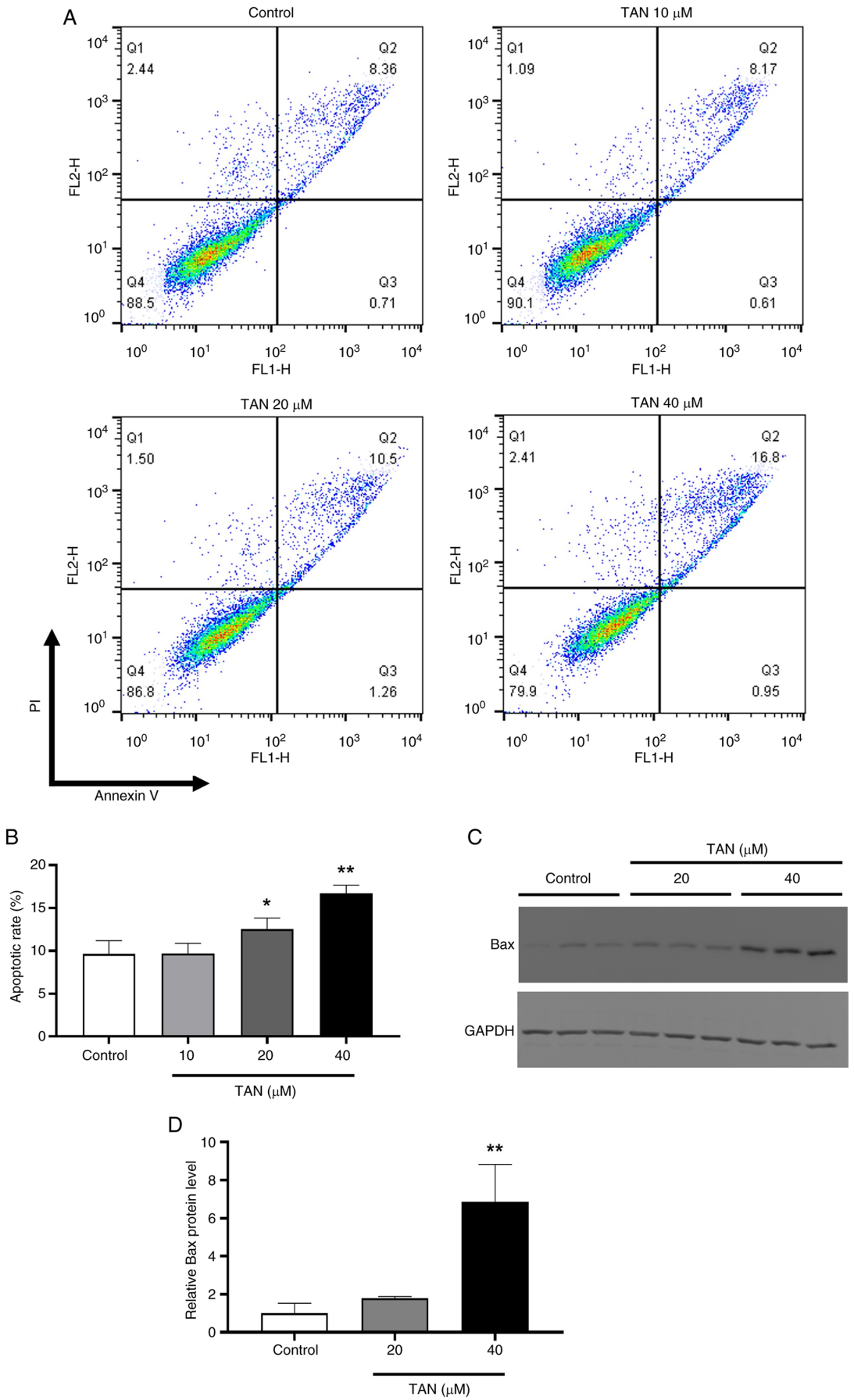

Figure 4. TAN induces the intrinsic apoptosis of CaSki cells. (A) Representative flow cytometry plots of Annexin V and PI staining showing apoptosis in CaSki cells following TAN treatment. (B) Quantification of apoptotic cell populations. (C) Representative western blot analysis images of Bax protein expression. (D) Semi-quantification of Bax protein expression by densitometric analysis normalized to GAPDH. Data are presented as the mean ± SD of technical triplicates. *P<0.05, **P<0.01 vs. control. PI, propidium iodide; TAN, tangeretin.

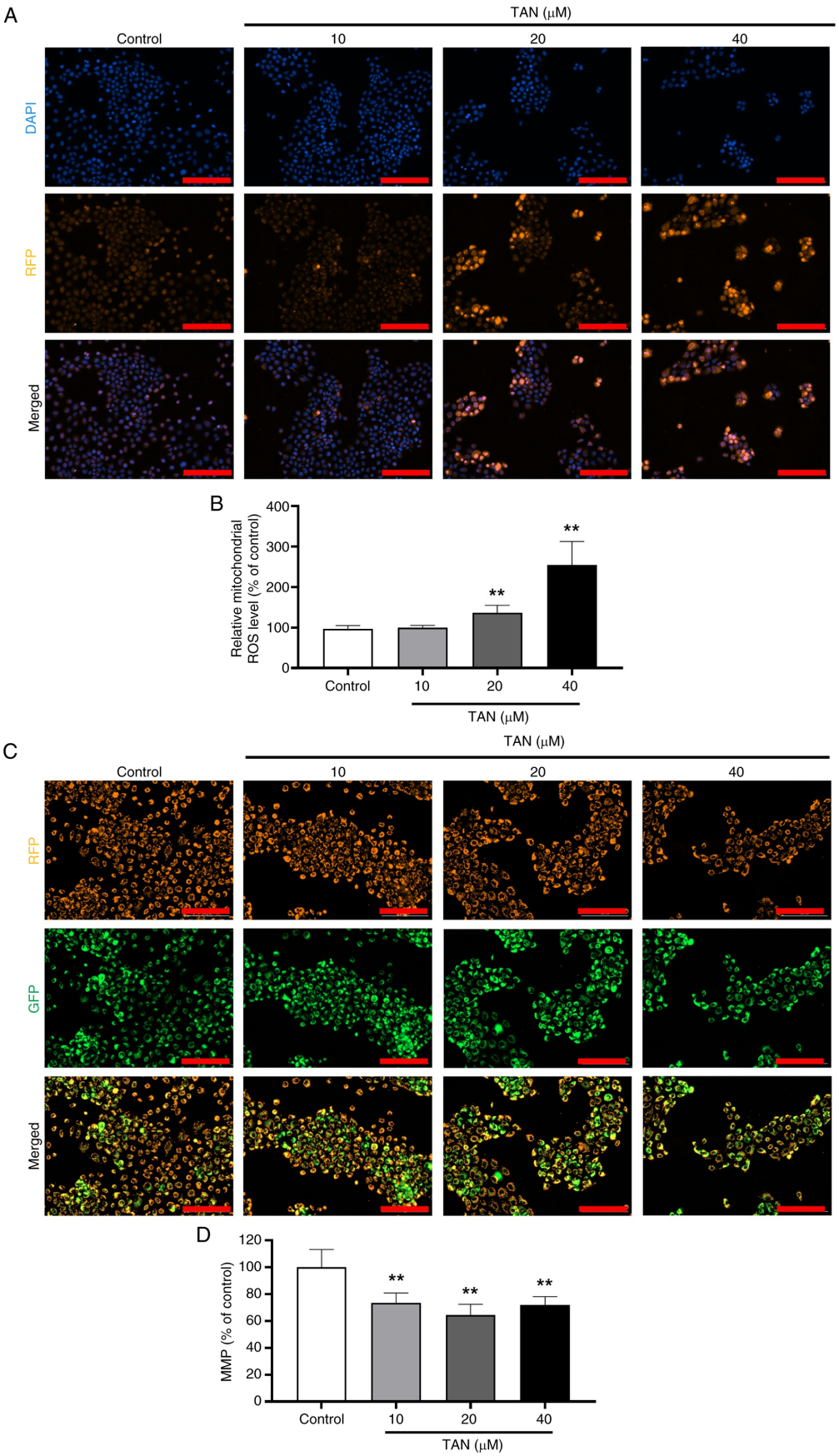

Figure 5. TAN increases mitochondrial oxidative stress and decreases in CaSki cells. (A) Representative fluorescence images of CaSki cells stained with MitoSOX™ and Hoechst 33342 to assess TAN-induced mitochondrial ROS accumulation. Scale bar, 200 μm. (B) Semi-quantification of mitochondrial ROS levels expressed as the fluorescence intensity ratio of MitoSOX to Hoechst 33342. (C) Representative fluorescence images of JC-1 staining showing TAN-induced changes in MMP. Scale bar, 200 μm. (D) Semi-quantification of MMP is expressed as the fluorescence intensity ratio of JC-1 dimers to JC-1 monomers. Data are presented as the mean ± SD of technical triplicates. **P<0.01 vs. control. MMP, mitochondrial membrane potential; ROS, reactive oxygen species; TAN, tangeretin.

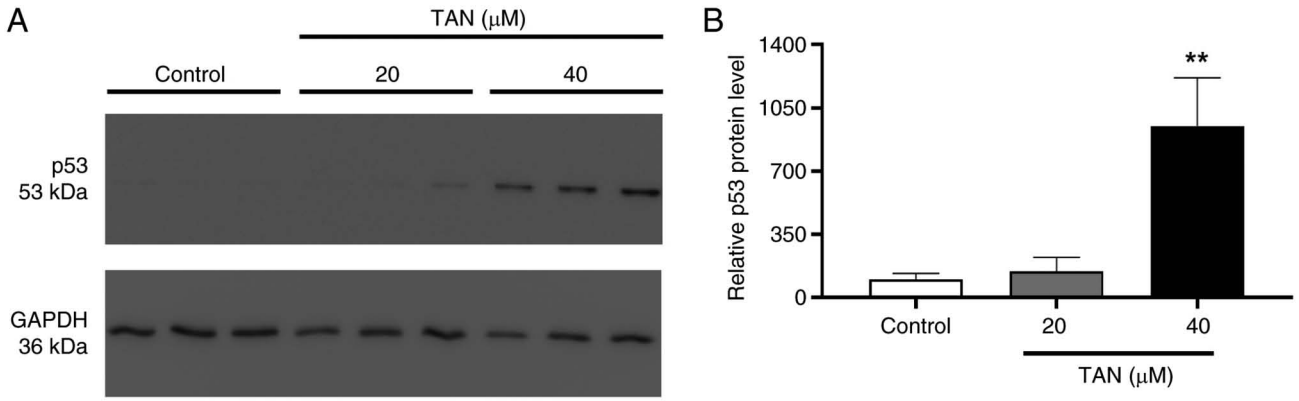

Figure 6. TAN upregulates the expression levels of a tumor suppressor protein in CaSki cells. (A) Western blotting was performed to detect the expression of p53, a tumor suppressor protein, after TAN treatment. (B) p53 protein expression was semi-quantified as the ratio of p53/GAPDH protein expression. Data are presented as the mean ± SD of technical triplicates. **P<0.01 vs. control. TAN, tangeretin.

TAN upregulates the expression levels of a tumor suppressor protein in CaSki cells. The tumor suppressor protein p53 is frequently inactivated or dysregulated in various cancer cell lines, and previous studies have reported that phytochemicals can modulate the expression of tumor suppressor proteins, including p53 (30-32). To evaluate the effect of TAN on p53 expression in CaSki cells, p53 protein levels were analyzed by western blotting (Fig. 6A). TAN treatment at 40 μM significantly increased p53 protein expression compared with that in the control group (Fig. 6B). These findings suggested that TAN treatment may be associated with increased p53 expression in CaSki cells.

Discussion

Phytochemicals, such as polyphenols, alkaloids and flavonoids, are plant-derived metabolites reported to exhibit a variety of bioactivities, including anticancer, antioxidant and anti-inflammatory effects (23,33,34). TAN is a methyl flavone-based phytochemical reported to have anticancer effects in previous studies (19,35,36). However, the anticancer effects of TAN in cervical cancer are still unclear and require further research. Therefore, the current study investigated the potential of TAN in the treatment of CaSki cervical cancer cells.

The present study demonstrated that TAN significantly reduced the viability and proliferation of CaSki cells, suggesting the induction of physiological and biochemical alterations in CaSki cells. The observed G_1 phase arrest induced by TAN was consistent with the findings of previous studies conducted in colon and breast cancer cells (37,38), suggesting that TAN may suppress the proliferation of CaSki cells through regulation of cell cycle progression. In addition, TAN upregulated the expression of the epithelial marker E-cadherin and reduced the migratory capacity of CaSki cells. Increased E-cadherin expression may be associated with suppression of epithelial-mesenchymal transition (EMT) through modulation of β-catenin-related signaling pathways, thereby reducing migration-associated phenotypic changes and metastatic potential (39,40). EMT is also associated with various malignant characteristics, including cancer stem cell (CSC) properties and resistance to apoptosis (41,42). Therefore, further studies are required to determine whether TAN influences additional EMT-associated processes, including CSC properties and apoptosis resistance.

Previous studies have reported that TAN can induce apoptosis in various cancer cell types through mitochondrial dysfunction and ROS-associated signaling pathways (19,26). Intrinsic apoptosis is triggered by mitochondrial dysfunction resulting from an imbalance in Bax/Bcl-2 expression and loss of MMP, leading to cytochrome *c* release (43,44). Increased mitochondrial ROS levels have also been recognized as an important factor associated with activation of the intrinsic apoptotic pathway (45,46). In the present study, increased Bax expression, elevated mitochondrial ROS levels and decreased MMP were observed following TAN treatment, suggesting the involvement of intrinsic apoptosis-associated mitochondrial dysfunction in CaSki cells. However, additional studies investigating intrinsic apoptosis-related signaling molecules, including caspase activation and cytochrome *c* release, are required to further clarify the underlying mechanisms. Furthermore, mitochondrial dysfunction has been reported to be closely associated with impaired electron transport chain activity, reduced adenosine triphosphate (ATP) production and alterations in mitochondria-dependent respiratory function (47). Therefore, further studies are needed to elucidate the effects of TAN on ATP production, mitochondrial metabolism and respiratory regulation in cancer cells.

Tumor suppressor proteins are frequently inactivated or functionally altered in numerous cancer cells and have therefore been extensively investigated as therapeutic targets (48). Among them, p53 and retinoblastoma proteins are known to be functionally suppressed by HPV oncoproteins, which serve a central role in the initiation and progression of cervical cancer (4,49,50). Therefore, modulation of tumor suppressor proteins such as p53 has been considered an important therapeutic target in cervical cancer research (51,52). In the present study, TAN treatment significantly increased p53 protein levels in CaSki cells; however, the precise mechanisms responsible for p53 regulation were not elucidated. In particular, changes in HPV16 E6/E7 mRNA and protein expression levels were not evaluated, and cycloheximide

chase experiments were not performed to determine whether TAN influences p53 protein stability through modulation of E6-mediated p53 degradation. Furthermore, p53 transcriptional activity and downstream target genes associated with cell cycle arrest and apoptosis, including p21, PUMA and NOXA, were not investigated. Functional validation experiments using p53 inhibitors, such as pifithrin-α or p53-specific small interfering RNA knockdown were also not performed. Therefore, it remains unclear as to whether the anticancer effects induced by TAN are directly dependent on p53 activation or whether TAN regulates HPV16 E6/E7 expression or activity to promote p53 stabilization. Further mechanistic studies are required to clarify the molecular mechanisms underlying TAN-induced p53 upregulation and to determine the functional contribution of p53 signaling to the anticancer effects of TAN.

Although TAN-induced G_1 phase arrest was observed in the present study, the molecular mechanisms underlying this effect were not fully investigated. In particular, key G_1/S transition-related regulatory proteins, including cyclin D1, CDK4/6, p21 and p27, were not evaluated. Therefore, additional studies are required to clarify the detailed molecular pathways associated with TAN-induced cell cycle arrest in cervical cancer cells. In addition, although increased mitochondrial ROS levels, Bax upregulation and decreased MMP were observed following TAN treatment, the present study did not directly establish ROS as a necessary upstream mediator of apoptosis. Rescue experiments using ROS scavengers, such as N-acetylcysteine or Mito-TEMPO, were not performed. Furthermore, apoptosis-related signaling molecules, including Bcl-2, cleaved caspase-3, cleaved caspase-9 and cytochrome *c* release, were not evaluated. Therefore, additional mechanistic studies are required to further clarify the ROS-associated intrinsic apoptotic pathways induced by TAN. In addition, given that the present study was limited to a single cervical cancer cell line, further investigations using multiple cervical cancer models with distinct biological characteristics, together with normal cervical epithelial cells, are warranted to establish the broader applicability and therapeutic potential of TAN. Moreover, although the present study demonstrated the anticancer potential of TAN in cervical cancer cells, its translational relevance remains to be further established. The concentrations of TAN used *in vitro* may not be physiologically achievable *in vivo* owing to pharmacokinetic limitations, including low bioavailability and limited systemic exposure (53). Therefore, further studies using appropriate animal models are required to evaluate the *in vivo* antitumor efficacy, systemic toxicity and pharmacokinetic profile of TAN under physiologically relevant conditions. A previous study suggested that TAN may exhibit relatively improved solubility and pharmacokinetic properties compared with other PMFs, including nobiletin, due to its structural characteristics (54). Nevertheless, TAN still possesses pharmacokinetic limitations, including relatively low bioavailability, which may restrict its clinical applicability. To overcome these limitations, studies have investigated various drug delivery systems, including self-microemulsifying drug delivery systems, nanoemulsions and nanoparticle-based formulations, to improve the stability and bioavailability of TAN, suggesting their potential utility for enhancing the therapeutic efficacy of TAN (53,55,56). Therefore, the incorporation of advanced drug delivery strategies may represent a promising approach to improve the translational potential and therapeutic applicability of TAN in cervical cancer.

Although several limitations remain to be addressed, the present study demonstrated that TAN treatment was associated with reduced proliferation, apoptosis-related changes and mitochondrial dysfunction in CaSki cervical cancer cells. These findings provide preliminary evidence supporting the potential anticancer activity of TAN, and may serve as a foundation for future mechanistic, pharmacological and preclinical studies in cervical cancer.

Acknowledgements

Not applicable.

Funding

This research was supported by the Regional Innovation System & Education (RISE) program through the Chungbuk Regional Innovation System & Education Center, funded by the Ministry of Education and the provincial government of Chungcheongbuk-do, Republic of Korea (grant no. 2025-RISE-11-014-03) and by Chungbuk National University BK21 program (2026). In addition, this work was supported by the National Research Foundation of Korea (NRF) grant funded by the Korean government (grant no. RS-2026-25486352) and the Sejong Fellowship through the NRF funded by the Ministry of Science and ICT (grant no. RS-2025-00557567).

Availability of data and materials

The data generated in the present study may be requested from the corresponding author.

Authors' contributions

HKL and KCC conceptualized the study. SHA, ZAB and HN developed the experimental methodology. HKL, ZAB and HN validated the experimental results. SHA performed the formal analysis. SHA, ZAB and HN conducted the investigation. SHA, ZAB and HN curated and organized the experimental data. SHA and ZAB wrote the original draft of the manuscript. HKL and KCC reviewed and edited the manuscript. SHA and ZAB prepared the figures and visualized the data. KCC supervised the study. HKL and KCC administered the project. KCC acquired the funding. SHA, ZAB and KCC confirm the authenticity of all the raw data. All authors read and approved the final manuscript.

Ethics approval and consent to participate

Not applicable.

Patient consent for publication

Not applicable.

Competing interests

The authors declare that they have no competing interests.

References

1. Bray F, Laversanne M, Sung H, Ferlay J, Siegel RL, Soerjomataram I and Jemal A: Global cancer statistics 2022: GLOBOCAN estimates of incidence and mortality worldwide for 36 cancers in 185 countries. CA Cancer J Clin 74: 229-263, 2024.
2. Áyen Á, Jiménez Martínez Y and Boulaiz H: Targeted gene delivery therapies for cervical cancer. Cancers (Basel) 12: 1301, 2020.
3. Yan H, Wang P, Yang F, Cheng W, Chen C, Zhai B and Zhou Y: Anticancer therapy-induced adverse drug reactions in children and preventive and control measures. Front Pharmacol 15: 1329220, 2024.
4. Ruttkay-Nedecky B, Jimenez Jimenez AM, Nejdl L, Chudobova D, Gumulec J, Masarik M, Adam V and Kizek R: Relevance of infection with human papillomavirus: the role of the p53 tumor suppressor protein and E6/E7 zinc finger proteins (review). Int J Oncol 43: 1754-1762, 2013.
5. Chew YC, Adhikary G, Wilson GM, Xu W and Eckert RL: Sulforaphane induction of p21(Cip1) cyclin-dependent kinase inhibitor expression requires p53 and Sp1 transcription factors and is p53-dependent. J Biol Chem 287: 16168-16178, 2012.
6. Fu H, Wang C, Yang D, Wei Z, Xu J, Hu Z, Zhang Y, Wang W, Yan R and Cai Q: Curcumin regulates proliferation, autophagy, and apoptosis in gastric cancer cells by affecting PI3K and P53 signaling. J Cell Physiol 233: 4634-4642, 2018.
7. Younas M, Hano C, Giglioli-Guivarc'h N and Abbasi BH: Mechanistic evaluation of phytochemicals in breast cancer remedy: Current understanding and future perspectives. RSC Adv 8: 29714-29744, 2018.
8. Hamdan AME, Alharthi FHJ, Alanazi AH, El-Emam SZ, Zaghlool SS, Metwally K, Albalawi SA, Abdu YS, Mansour RE, Salem HA, *et al*: Neuroprotective effects of phytochemicals against aluminum chloride-induced Alzheimer's disease through ApoE4/LRP1, Wnt3/β-Catenin/GSK3β, and TLR4/NLRP3 pathways with physical and mental activities in a rat model. Pharmaceuticals (Basel) 15: 1008, 2022.
9. Sohel M, Aktar S, Biswas P, Amin MA, Hossain MA, Ahmed N, Mim MIH, Islam F and Mamun AA: Exploring the anti-cancer potential of dietary phytochemicals for the patients with breast cancer: A comprehensive review. Cancer Med 12: 14556-14583, 2023.
10. Paudel S, Mishra N and Agarwal R: Phytochemicals as immunomodulatory molecules in cancer therapeutics. Pharmaceuticals (Basel) 16: 1652, 2023.
11. Chen S, Wang X, Cheng Y, Gao H and Chen X: A review of classification, biosynthesis, biological activities and potential applications of flavonoids. Molecules 28: 4982, 2023.
12. Hosseinzadeh A, Poursoleiman F, Biregani AN and Esmailzadeh A: Flavonoids target different molecules of autophagic and metastatic pathways in cancer cells. Cancer Cell Int 23: 114, 2023.
13. Kopustinskiene DM, Jakstas V, Savickas A and Bernatoniene J: Flavonoids as anticancer agents. Nutrients 12: 457, 2020.
14. An JP, Liu X, Kim D, Madden R and Wang Y: Comprehensive analysis of polymethoxyflavone metabolism in orange peel using an animal model. RSC Adv 15: 38189-38200, 2025.
15. Wang Y, Mou Y, Lu S, Xia Y and Cheng B: Polymethoxylated flavonoids in citrus fruits: Absorption, metabolism, and anticancer mechanisms against breast cancer. PeerJ 12: e16711, 2024.
16. Raza W, Luqman S and Meena A: Prospects of tangeretin as a modulator of cancer targets/pathways. Pharmacol Res 161: 105202, 2020.
17. Hung WL, Chang WS, Lu WC, Wei GJ, Wang Y, Ho CT and Hwang LS: Pharmacokinetics, bioavailability, tissue distribution and excretion of tangeretin in rat. J Food Drug Anal 26: 849-857, 2018.
18. Dey DK, Chang SN, Vadlamudi Y, Park JG and Kang SC: Synergistic therapy with tangeretin and 5-fluorouracil accelerates the ROS/JNK mediated apoptotic pathway in human colorectal cancer cell. Food Chem Toxicol 143: 111529, 2020.
19. Dong Y, Cao A, Shi J, Yin P, Wang L, Ji G, Xie J and Wu D: Tangeretin, a citrus polymethoxyflavonoid, induces apoptosis of human gastric cancer AGS cells through extrinsic and intrinsic signaling pathways. Oncol Rep 31: 1788-1794, 2014.
20. Xie Y, Feng SL, He F, Yan PY, Yao XJ, Fan XX, Leung EL and Zhou H: Down-regulating Nrf2 by tangeretin reverses multiple drug resistance to both chemotherapy and EGFR tyrosine kinase inhibitors in lung cancer. Pharmacol Res 186: 106514, 2022.
21. Varankar SS and Bapat SA: Migratory metrics of wound healing: A quantification approach for in vitro scratch assays. Front Oncol 8: 633, 2018.
22. Ibrahim SM, Bakhashab S, Ilyas AM, Pushparaj PN, Karim S, Khan JA, Abuzenadah AM, Chaudhary AG, Al-Qahtani MH and Ahmed F: WYE-354 restores Adriamycin sensitivity in multidrug-resistant acute myeloid leukemia cell lines. Oncol Rep 41: 3179-3188, 2019.
23. Atchan APN, Monthe OC, Tchamgoue AD, Singh Y, Shivashankara ST, Selvi MK, Agbor GA, Magni P, Piazza S, Manjappara UV, *et al*: Anti-inflammatory, antioxidant activities, and phytochemical characterization of edible plants exerting synergistic effects in human gastric epithelial cells. Antioxidants (Basel) 12: 591, 2023.
24. Lin JJ, Huang CC, Su YL, Luo HL, Lee NL, Sung MT and Wu YJ: Proteomics analysis of tangeretin-induced apoptosis through mitochondrial dysfunction in bladder cancer cells. Int J Mol Sci 20: 1017, 2019.
25. Zhang X, Zheng L, Sun Y, Wang T and Wang B: Tangeretin enhances radiosensitivity and inhibits the radiation-induced epithelial-mesenchymal transition of gastric cancer cells. Oncol Rep 34: 302-310, 2015.
26. Jeoung YH, Lee HK, Ahn SH, Bhutta ZA and Choi KC: Tangeretin induces apoptosis and cell cycle arrest in thyroid cancer cells. Toxicol Res 41: 477-488, 2025.
27. Surichan S, Arroo RR, Tsatsakis AM and Androutsopoulos VP: Tangeretin inhibits the proliferation of human breast cancer cells via CYP1A1/CYP1B1 enzyme induction and CYP1A1/CYP1B1-mediated metabolism to the product 4' hydroxy tangeretin. Toxicol In Vitro 50: 274-284, 2018.
28. Schegoleva AA, Khozyainova AA, Gerashchenko TS, Zhuikova LD and Denisov EV: Metastasis prevention: Targeting causes and roots. Clin Exp Metastasis 39: 505-519, 2022.
29. Ting YW, Chiou YS, Pan MH, Ho CT and Huang QR: In vitro and in vivo anti-cancer activity of tangeretin against colorectal cancer was enhanced by emulsion-based delivery system. J Funct Foods 15: 264-273, 2015.
30. Li X, Li Q, Huang Y, Zhou H, Yang Q and Kong L: Quercetin, a natural dietary flavonoid, emerges a novel USP7 inhibitor with anti-colorectal cancer effects. Biol Pharm Bull 48: 1485-1492, 2025.
31. Kang KA, Piao MJ, Hyun YJ, Zhen AX, Cho SJ, Ahn MJ, Yi JM and Hyun JW: Luteolin promotes apoptotic cell death via upregulation of Nrf2 expression by DNA demethylase and the interaction of Nrf2 with p53 in human colon cancer cells. Exp Mol Med 51: 1-14, 2019.
32. Jung EJ, Lee WS, Paramanantham A, Kim HJ, Shin SC, Kim GS, Jung JM, Ryu CH, Hong SC, Chung KH and Kim CW: p53 Enhances Artemisia annua L. Polyphenols-induced cell death through upregulation of p53-dependent targets and cleavage of PARP1 and lamin A/C in HCT116 colorectal cancer cells. Int J Mol Sci 21: 9315, 2020.
33. Alshehri A, Ahmad A, Tiwari RK, Ahmad I, Alkhathami AG, Alshahrani MY, Asiri MA, Almeleebia TM, Saeed M, Yadav DK and Ansari IA: In vitro evaluation of antioxidant, anticancer, and anti-inflammatory activities of ethanolic leaf extract of Adenium obesum. Front Pharmacol 13: 847534, 2022.
34. Pandey BP, Adhikari K, Pradhan SP, Shin HJ, Lee EK and Jung HJ: In-vitro antioxidant, anti-cancer, and anti-inflammatory activities of selected medicinal plants from western Nepal. Futur J Pharm Sci 6: 75, 2020.
35. Ko YC, Choi HS, Liu R, Kim JH, Kim SL, Yun BS and Lee DS: Inhibitory effects of tangeretin, A citrus peel-derived flavonoid, on breast cancer stem cell formation through suppression of Stat3 signaling. Molecules 25: 2599, 2020.
36. Zhu WB, Xiao N and Liu XJ: Dietary flavonoid tangeretin induces reprogramming of epithelial to mesenchymal transition in prostate cancer cells by targeting the PI3K/Akt/mTOR signaling pathway. Oncol Lett 15: 433-440, 2018.
37. Morley KL, Ferguson PJ and Koropatnick J: Tangeretin and nobiletin induce G1 cell cycle arrest but not apoptosis in human breast and colon cancer cells. Cancer Lett 251: 168-178, 2007.
38. Pan MH, Chen WJ, Lin-Shiau SY, Ho CT and Lin JK: Tangeretin induces cell-cycle G1 arrest through inhibiting cyclin-dependent kinases 2 and 4 activities as well as elevating Cdk inhibitors p21 and p27 in human colorectal carcinoma cells. Carcinogenesis 23: 1677-1684, 2002.

39. Hui San S and Ching Ngai S: E-cadherin re-expression: Its potential in combating TRAIL resistance and reversing epithelial-to-mesenchymal transition. Gene 909: 148293, 2024.
40. Lin WH, Cooper LM and Anastasiadis PZ: Cadherins and catenins in cancer: Connecting cancer pathways and tumor microenvironment. Front Cell Dev Biol 11: 1137013, 2023.
41. Mani SA, Guo W, Liao MJ, Eaton EN, Ayyanan A, Zhou AY, Brooks M, Reinhard F, Zhang CC, Shipitsin M, *et al*: The epithelial-mesenchymal transition generates cells with properties of stem cells. Cell 133: 704-715, 2008.
42. Vega S, Morales AV, Ocaña OH, Valdés F, Fabregat I and Nieto MA: Snail blocks the cell cycle and confers resistance to cell death. Genes Dev 18: 1131-1143, 2004.
43. Mustafa M, Ahmad R, Tantry IQ, Ahmad W, Siddiqui S, Alam M, Abbas K, Moinuddin, Hassan MI, Habib S and Islam S: Apoptosis: A comprehensive overview of signaling pathways, morphological changes, and physiological significance and therapeutic implications. Cells 13: 1838, 2024.
44. Vogler M, Braun Y, Smith VM, Westhoff MA, Pereira RS, Pieper NM, Anders M, Callens M, Vervliet T, Abbas M, *et al*: The BCL2 family: From apoptosis mechanisms to new advances in targeted therapy. Signal Transduct Target Ther 10: 91, 2025.
45. Heo JW, No MH, Park DH, Kang JH, Seo DY, Han J, Neufer PD and Kwak HB: Effects of exercise on obesity-induced mitochondrial dysfunction in skeletal muscle. Korean J Physiol Pharmacol 21: 567-577, 2017.
46. Roy MJ, Vom A, Czabotar PE and Lessene G: Cell death and the mitochondria: Therapeutic targeting of the BCL-2 family-driven pathway. Br J Pharmacol 171: 1973-1987, 2014.
47. Khan T, Waseem R, Zehra Z, Aiman A, Bhardwaj P, Ansari J, Hassan MI and Islam A: Mitochondrial dysfunction: Pathophysiology and mitochondria-targeted drug delivery approaches. Pharmaceutics 14: 2657, 2022.
48. Wang H, Guo M, Wei H and Chen Y: Targeting p53 pathways: Mechanisms, structures, and advances in therapy. Signal Transduct Target Ther 8: 92, 2023.
49. Rastogi N, Duggal S, Singh SK, Porwal K, Srivastava VK, Maurya R, Bhatt ML and Mishra DP: Proteasome inhibition mediates p53 reactivation and anti-cancer activity of 6-gingerol in cervical cancer cells. Oncotarget 6: 43310-43325, 2015.
50. Zhao X, Sun W, Ren Y and Lu Z: Therapeutic potential of p53 reactivation in cervical cancer. Crit Rev Oncol Hematol 157: 103182, 2021.
51. Wang JCK, Baddock HT, Mafi A, Foe IT, Bratkowski M, Lin TY, Jensvold ZD, Preciado López M, Stokoe D, Eaton D, *et al*: Structure of the p53 degradation complex from HPV16. Nat Commun 15: 1842, 2024.
52. Zou J, Li Y, Chen T and Zhu C: An E7-retinoblastoma protein pathway mechanism may account for the higher carcinogenic ability of HPV16 over HPV58 in cervical cancer. Transl Cancer Res 13: 1876-1886, 2024.
53. Wang W, Jia T, Zhang Y and Zhou Y: Progress of researches on pharmacological effects and bioavailability of tangeretin. J Oleo Sci 74: 13-23, 2025.
54. Woo SH, Park IC, Park MJ, Lee HC, Lee SJ, Chun YJ, Lee SH, Hong SI and Rhee CH: Arsenic trioxide induces apoptosis through a reactive oxygen species-dependent pathway and loss of mitochondrial membrane potential in HeLa cells. Int J Oncol 21: 57-63, 2002.
55. Elhennawy MG and Lin HS: Determination of tangeretin in rat plasma: Assessment of its clearance and absolute oral bioavailability. Pharmaceutics 10: 3, 2017.
56. Hu Y, Liu F, Pang J, McClements DJ, Zhou Z, Li B and Li Y: Biopolymer additives enhance tangeretin bioavailability in emulsion-based delivery systems: an in vitro and in vivo study. J Agric Food Chem 69: 730-740, 2021.